Neuron, Vol. 48, 1025–1037, December 22, 2005, Copyright ©2005 by Elsevier Inc. DOI 10.1016/j.neuron.2005.10.029

A Specialized Subclass of Interneurons Mediates Dopaminergic Facilitation of Amygdala Function

Anne Marowsky,[1] Yuchio Yanagawa,[2,3] Kunihiko Obata,[4] and Kaspar Emanuel Vogt[1,*]
[1] Institute for Pharmacology and Toxicology
University of Zurich
Winterthurerstrasse 190
CH-8057 Zurich
Switzerland
[2] Department of Genetic and Behavioural Neuroscience
Gunma University Graduate School of Medicine
Maebashi
Japan
[3] CREST and SORST
Japan Science and Technology Corporation
Kawaguchi
Japan
[4] Neuronal Circuit Mechanisms Research Group
RIKEN Brain Science Institute
Wako
Japan

Summary

The amygdala is under inhibitory control from the cortex through the activation of local GABAergic interneurons. This inhibition is greatly diminished during heightened emotional states due to dopamine release. However, dopamine excites most amygdala interneurons, suggesting that this dopaminergic gate may be mediated by an unknown subpopulation of interneurons. We hypothesized that this gate is mediated by paracapsular intercalated cells, a subset of interneurons that are innervated by both cortical and mesolimbic dopaminergic afferents. Using transgenic mice that express GFP in GABAergic interneurons, we show that paracapsular cells form a network surrounding the basolateral complex of the amygdala. We found that they provide feedforward inhibition into the basolateral and the central amygdala. Dopamine hyperpolarized paracapsular cells through D1 receptors and substantially suppressed their excitability, resulting in a disinhibition of the basolateral and central nuclei. Suppression of the paracapsular system by dopamine provides a compelling neural mechanism for the increased affective behavior observed during stress or other hyperdopaminergic states.

Introduction

The amygdala plays a crucial role in producing emotionally appropriate behavior in response to sensory input, in particular to threatening stimuli (LeDoux, 2000). For this process, an intact inhibitory system is essential as illustrated by the fact that selective blocking of inhibition (e.g., by infusion of $GABA_A$ receptor blockers in the amygdala) produces an uncontrolled anxiety-like state (Sanders and Shekhar, 1995). Previous findings indicate that cortical afferents drive inhibition in the amygdala by activating local interneurons (Lang and Pare, 1998; Le Gal LaSalle et al., 1978), resulting in suppressed output from the basolateral amygdala (BLA, consisting of the lateral, basolateral, and basomedial nuclei) (Rosenkranz and Grace, 2002) and the central amygdala (CeA) (Quirk et al., 2003). However, in situations in which an emotional response is important, cortically mediated inhibition must be lifted to facilitate amygdala function. Several lines of evidence suggest that the modulatory neurotransmitter dopamine (DA) may act as switch between the cortically controlled and the disinhibited states of the amygdala: (1) DA is increased under stress in the amygdala (Inglis and Moghaddam, 1999; Yokoyama et al., 2005), thus available in emotionally charged situations; (2) DA produces disinhibition in the BLA (Grace and Rosenkranz, 2002; Rosenkranz and Grace, 1999); (3) release of DA enhances amygdala-related behavior (Borowski and Kokkinidis, 1998), whereas inhibition of the dopaminergic system depresses amygdala-related behavior such as fear learning and the expression of fear (Greba and Kokkinidis, 2000; Lamont and Kokkinidis, 1998; Nader and LeDoux, 1999).

DA receptors can be classified into two main groups with the DA D1 receptors comprising the subtypes D1 and D5, and the DA D2 receptors comprising the subtypes D2, D3, and D4 (Missale et al., 1998). In particular DA D1 receptors appear to be essential for disinhibition of the amygdala, as prefrontal cortical control over the amygdala is strongly reduced through DA D1 receptor activation (Rosenkranz and Grace, 2002). Further evidence for the importance of the DA D1 receptor system stems from behavioral studies, in which activation of these receptors by systemic application of the selective agonists SKF38393 augments both fear learning and expression (Borowski and Kokkinidis, 1998), and systemic or focal application of the DA D1 receptor antagonist SCH 23390 (Greba and Kokkinidis, 2000; Inoue et al., 2000; Meloni and Davis, 1999) blocks either the acquisition or both acquisition and expression of fear.

On a cellular level, disinhibition of the BLA can either result from reduced excitatory input to interneurons or from a direct suppression of amygdala interneuron excitability. However, interneurons within the BLA were shown to be depolarized by DA or DA D1 receptor agonists, increasing rather than reducing inhibitory activity (Kröner et al., 2004; Rosenkranz and Grace, 2002). This raises the question as to whether a subpopulation of amygdala interneurons exists that is differently modulated by DA and mediates cortical control of the amygdala. In the rat amygdala, the so-called paracapsular intercalated cells (pcs) (Alheid et al., 1995; Millhouse, 1986) receive the densest afferents from the mesencephalic DAergic system with a high number of somatic and perisomatic synapses and show the highest levels of DA D1 receptor immunoreactivity and DA D1 receptor mRNA (Asan, 1998; Fuxe et al., 2003). Functional data on these interneurons is scant except for the subgroup forming an inhibitory gate between BLA and CeA presumably under cortical control (Pare et al., 2003; Royer

*Correspondence: kvogt@pharma.unizh.ch

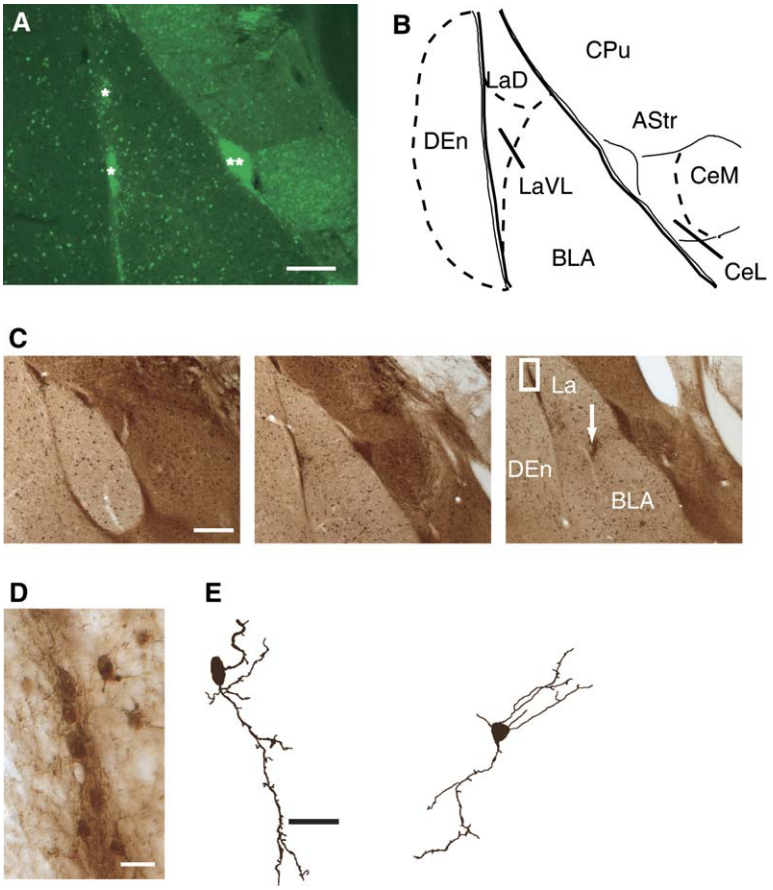

Figure 1. Location and Morphology of Paracapsular Intercalated Cells in GAD-GFP Mice

(A) Paracapsular intercalated cells (pcs) are located at both borders of the lateral and basolateral amygdala. They can be identified as clusters (* lateral pcs [lpcs] and ** medial pcs [mpcs]) of densely packed fluorescent cells in acute brain slices from GAD-GFP mice. Scale bar: 200 μm.

(B) Schematic with: LaD, lateral amygdala dorsal nucleus; LaVL, lateral amygdala ventero-lateral nucleus; BLA, basolateral amygdala; CPu, caudate putamen; Astr, amygdalostriatal transition area; CeM, medial division of the central nucleus; CeL, lateral division of the central nucleus; DEn, dorsal endopiriform nucleus.

(C) DAB staining against GFP in fixated slices obtained from GAD-GFP mice; GABAergic cells are dark brown. *Left,* rostral section: intercalated cells and their dendrites form a continuous shell around the BLA. *Middle,* intermediate section: pcs are found as dense clusters along the external and intermediate capsule. *Right,* caudal section: the two clusters are linked by strands of small interneurons (downward arrow). Rectangle marks the region enlarged in (D). Scale bar: 200 μm.

(D) Inset from (C), note the dense network of dendrites running in the dorso-ventral direction along and within the external capsule. Scale bar: 20 μm.

(E) Biocytin-filled, small, sparsely spined interneurons; lpcs are typically more spindle shaped, whereas mpcs are oval or round. Scale bar: 20 μm.

et al., 1999). For the second prominent subgroup, located along the external capsule, physiological data are largely missing.

Given the occurrence of pcs along the fiber bundles carrying cortical afferents together with their dense dopaminergic innervation, we hypothesized that these cells are substantially involved in mediating the prominent cortical feedforward inhibition and its modulation by DA observed in the amygdala.

Using mice that express GFP in GABAergic interneurons (Tamamaki et al., 2003), we were able to identify pcs in acute brain slices and study their connectivity and response to DA. Here we demonstrate that pcs form an interconnected system provide feedforward inhibition into the BLA complex and the CeA and show a modulation by DA and DA D1 agonists that is not found in other neurons in the amygdala.

Results

Morphology of Paracapsular Intercalated Cells

GAD-GFP mice (Tamamaki et al., 2003) express green fluorescent protein (GFP) under the control of the promotor for GAD67, a key enzyme for the synthesis of γ-aminobutyric acid (GABA). With help of these mice, two types of interneurons could be distinguished in the amygdala: "classical" interneurons that occur loosely scattered within the BLA and densely packed clusters of smaller interneurons that are located along the external capsule and along the medial border between the BLA and central amygdala (Figures 1A and 1C). Consistent with location and morphology, we identified the latter as pcs (Alheid et al., 1995; Millhouse, 1986) with a lateral (lpcs [*]) and a medial (mpcs [**]) subdivision. These subdivisions were linked by a cell band stretching across the BLA (Figure 1C, downward arrow), presumably constituting a third group of pcs. Characteristic for pcs is their small size (5–8 μm in diameter, n = 27), a poorly developed dendritic tree, and their occurrence in tightly packed nuclei (Figures 1D and 1E). A three-dimensional reconstruction of the pc system revealed that they form an inhibitory sheath around the BLA (Supplemental Data available with this article online). In immunohistochemical studies, subsets of BLA interneurons were immunopositive for typical interneuron markers (calbindin, calretinin, parvalbumin, NPY, cholecystokinin, somatostatin), yet none of these markers labeled pcs (data not shown).

Functional Characterization of pcs

In a first set of experiments, we examined the electrophysiological properties of lpcs, mpcs, and classical BLA interneurons as shown in Table 1. Compared to classical interneurons, pcs exhibited broader spikes, less pronounced afterhyperpolarizations, and lower sustained spike frequencies. These features were especially prominent in lpcs; in fact, their spiking pattern was reminiscent of the one observed in pyramidal cells, whereas the firing pattern of mpcs more closely resembled the one observed in other BLA interneurons (Figures 2A–2D). The

Table 1. Electrophysiological Properties of Lateral and Medical Paracapsular Intercalated Cells and Interneurons within the Basolateral Amygdala

	lpc			mpc			IN BLA			
	avg	SEM	n	avg	SEM	n	avg	SEM	n	
Parameter										
RMP (mV)	−78	1.3	44	−78	1.6	36	−77	2.8	25	lpc ≈ mpc ≈ IN BLA
Rin (MOhm)	865	31	44	657	49	36	341	37	25	lpc > mpc > IN BLA
Cap (pF)	57.1	1.2	44	59	3.1	36	93	7.2	25	lpc ≈ mpc < IN BLA
peak f (Hz)	19.9	1.2	43	24.8	1.9	36	45.4	4	25	lpc ≈ mpc < IN BLA
sustained f (Hz)	14.8	0.35	43	19.4	1	36	39.5	0.6	25	lpc < mpc < IN BLA
f adapt (rel)	0.75	0.03	43	0.78	0.05	36	0.8	0.02	25	lpc ≈ mpc ≈ IN BLA
hw first (ms)	1.7	0.032	43	1.2	0.034	36	1.2	0.09	25	lpc > mpc ≈ IN BLA
hw sust (ms)	2.85	0.053	43	1.9	0.093	36	1.37	0.037	25	lpc > mpc > IN BLA
AP first (mV)	67	1.4	43	68	1.4	36	70	1.9	25	lpc ≈ mpc ≈ IN BLA
AP sust (mV)	51	0.8	43	54	1.2	36	60	0.5	25	lpc < mpc < IN BLA

We measured resting membrane potential (RMP), input resistance (Rin), whole-cell capacitance (Cap), peak firing frequency—first three action potentials (peak f), sustained firing frequency—last four action potentials (sustained f), frequency adaptation (sustained frequency divided by the peak frequency), action potential half-width of the first action potential (hw first), action potential half-width of the last action potential (hw sust), amplitude of the action potential from the beginning of the upstroke to the peak for the first action potential (AP first) and for the last action potential (AP sust). Average values (avg), standard error of the mean (SEM), and the number of recordings (n) are given. Statistics were computed using one-way ANOVAs and post-hoc Bonferroni tests. > or < indicate statistically significant differences; ≈ indicates no significant difference.

passive membrane properties of pcs such as input resistance and whole-cell capacitance were typical for small neurons, with the lpcs possessing even higher input resistance and lower whole-cell capacitance than mpcs (see Table 1).

Lpcs Receive Excitatory Cortical Input and Project onto BLA Pyramidal Cells

Previous anatomical and electrophysiological studies demonstrated that mpcs receive excitatory input from BLA projection cells (Royer et al., 1999; Smith and Pare, 1994) and send projections to CeA neurons, providing feedforward inhibition of the CeA. In addition, studies by Quirk et al. (2003) and Berretta et al. (2005) imply cortical activation of mpcs. As lpcs are located in close proximity to the external capsule, we investigated whether they are also innervated by cortical afferents. Individual lpcs were recorded in current-clamp mode, while cortical afferents were activated through a bipolar platinum-iridium electrode placed onto the external capsule (Humeau et al., 2003). Stimulation of the fiber bundle resulted in EPSPs of sufficient size to fire lpcs (n = 5) (Figures 2E and 2F). To confirm the specificity of cortical innervation, the external capsule was severed with the result that stimulation distal of the cut no longer evoked any synaptic response in the lpc, though proximal stimulation still generated robust excitation (n = 4) (Figures 2G and 2H). Either proximal stimulation or increased stimulation intensity recruited IPSPs in addition to EPSPs, indicating that lpcs receive excitatory cortical innervation and lateral inhibition from other interneurons, reminiscent of the situation in mpcs (Royer et al., 1999).

A first indication concerning their target cells was obtained by biocytin-filled lpcs, which send axonal collaterals into the BLA. To verify functional connectivity, we recorded from connected lpc-BLA projection cell pairs. Lpcs were recorded in whole-cell current-clamp mode, and presynaptic action potentials were elicited by brief (1 ms) current injections. We recorded from 134 lpc-BLA projection cell pairs; we detected synaptic connections in 7 of these. The amplitude of unitary IPSCs (uIPSCs) was small (16 ± 1.7 pA), and their kinetics were slow (rise time: 5.0 ± 0.7 ms, decay time: 46.8 ± 13.1 ms) (Figures 3B and 3C). Signal size and kinetics strongly imply dendritic, rather than somatic synaptic contacts between lpcs and BLA principal cells, which is in accordance with the distal axo-dendritic contact found in biocytin-filled cell pairs (Figure 3A). Such modest IPSCs may only have limited inhibitory impact on their targets, but if multiple lpcs from a single cluster project to a single BLA principal cell, this could considerably enhance the inhibitory effectiveness of lpcs. We tested this hypothesis by stimulating lpc clusters with an extracellular stimulus electrode and recording IPSCs from a single BLA projection cell (n = 4) (Figure 3D). To ensure local activation of lpcs, an ACFS-filled glass electrode with a small tip was used and recordings were performed in the presence of kynurenate (3 mM). In all experiments, increasing the stimulation current resulted in a slowly growing inhibitory response due to gradual recruitment of lpcs and multiple innervation of the target cell by lpcs (Figures 3E and 3F).

So far we have shown that lpcs are activated by cortical afferents and project to BLA projection cells. However, some BLA interneurons are also cortically activated (Lang and Pare, 1998; Szinyei et al., 2000), raising the question as to which amount of feedforward inhibition is mediated by lpcs. To assess their contribution to cortical feedforward inhibition, we stimulated afferents in the external capsule while selectively blocking excitatory synaptic transmission onto lpcs with brief (1–2 s) focal puffs of the AMPA/kainate receptor blocker NBQX (1 mM) (Figures 3G–3J) (Royer et al., 1999). These puffs caused a transient reduction in the IPSC amplitude of BLA projection cells that were recorded in the vicinity of the superfused cluster (Figures 3H and 3I). On average the IPSC amplitude was reduced to 31% ± 7% of pre-application values (n = 5, $p < 0.05$) (Figure 3J), showing that the predominant part of cortical feedforward inhibition on BLA pyramidal cells is carried by lpcs.

Since cortically mediated inhibition is strongly sensitive to DA as shown by Rosenkranz and Grace (2002), we next studied the response of the paracapsular system to DA.

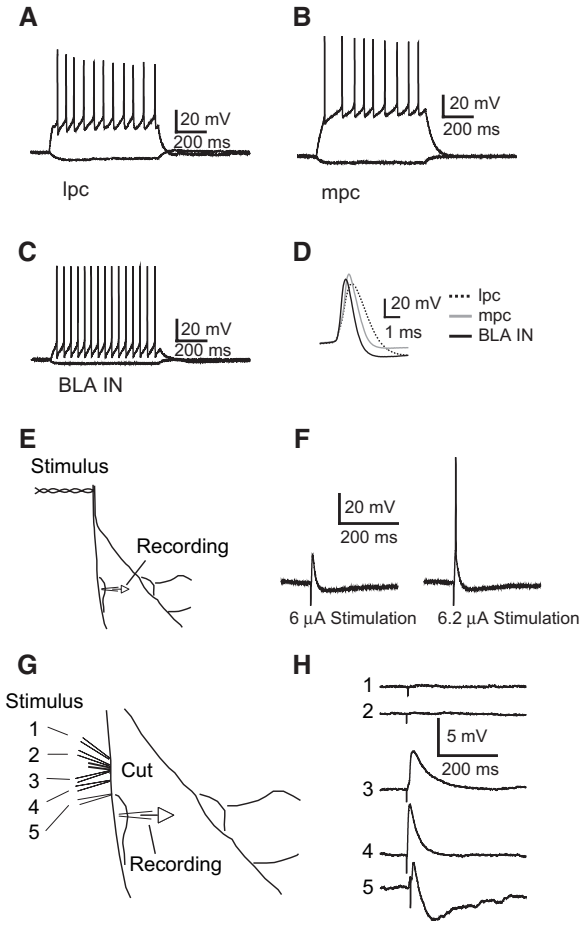

Figure 2. Basic Physiology of pcs and Innervation Pattern of Lpcs

(A–C) Characteristic spiking patterns of the different GABAergic interneurons in the amygdala. (A) Response of a lpc to somatic current injections of −10 pA and 50 pA, (B) of an mpc to −10 pA and 60 pA current injection, and (C) of a classical interneuron within the BLA to −10 pA and 90 pA current injection.

(D) Enlarged plot of the first action potential from the three cell types—lpcs (dotted line), mpcs (gray line), and BLA interneuron (black line).

(E and F) Lpcs can be activated through cortical afferents. (E) Schematic of the electrode placement; cortical afferents were stimulated with a bipolar platinum-iridium wire electrode. (F) Example of a whole-cell current-clamp recording from a lpc with short-latency EPSP/IPSP response to a subthreshold 6 μA stimulation (left) and subsequent action potential firing when stimulating at 6.2 μA (right).

(G and H) Severing the external capsule interrupts excitatory afferents. (G) Schematic drawing of the selective cut placed in the external capsule and the different positions (1–5) of the monopolar glass stimulus electrode. The electrode was sequentially positioned at the numbered sites and an identical stimulus was applied. (H) Whole-cell current-clamp recordings from a lpc. Distal to the cut through the external capsule, no postsynaptic response could be evoked (1 and 2). Immediately proximal to the cut, the same stimulus strengths evoked an EPSP (3). Moving closer to the recorded cell with the stimulus electrode results in larger EPSPs and the additional recruitment of IPSPs (4 and 5). Traces are averages of eight to ten individual responses per stimulation site in one cell.

Dopaminergic Modulation of pcs

Consistent with previous data obtained in the rat (Asan, 1998), dense tyrosine hydroxylase-positive plexuses were found within lpc and mpc clusters in GAD-GFP mice (Figures 4A and 4B). We assessed the physiological effect of this prominent innervation by applying DA (20–30 μM DA was used throughout the study) while recording from a pc (mpc and lpc) held in current-clamp. In lpcs, bath application of DA caused a hyperpolarization of the resting membrane potential (RMP) from −71.6 ± 1.3 mV to −76.4 ± 1.4 mV (n = 8, $p < 0.01$) and in mpcs from −73.3 ± 1.3 mV to −77.9 ± 1.4 mV (n = 12, $p < 0.01$) (Figure 4C). The effect was reversible upon washout. No significant difference in the amount of hyperpolarization was observed between lpcs and mpcs, and therefore data of both groups were pooled for subsequent experiments.

To examine whether DA directly acts on pc membrane potential and to study the ensuing effect on pc excitability, we repeated the experiments under complete block of ionotropic glutamatergic and GABAergic synaptic transmission (3 mM kynurenate, 100 μM picrotoxin) and evoked action potentials via somatic current injections. Bath application of DA hyperpolarized pcs by −4.7 ± 0.4 mV (−74.5 ± 1.2 mV to −79.3 ± 1.1 mV) (n = 20, $p < 0.01$), accompanied by a reduction of input resistance (810 ± 100 MΩ to 564 ± 45 MΩ, n = 20, $p < 0.01$) and of evoked spikes from 6.5 ± 1.1 to 1.6 ± 0.6 per trial (n = 20, $p < 0.01$) (Figures 4E and 4F). In another series of experiments, we applied DA in the presence of TTX (1 μM), which completely abolished network activity in the slice, and again measured a significant hyperpolarization (−4.6 ± 0.4 mV, n = 10, $p < 0.01$). As synaptic activity was not necessary for hyperpolarization, and activation of DA receptors on these cells led to a marked decrease in input resistance, we concluded that DA attenuates the excitability of pcs via a direct postsynaptic effect by increasing a hyperpolarizing conductance. In contrast to the inhibitory effect of DA on pcs, we found that classical BLA interneurons were invariably depolarized by DA (−74.4 ± 1.6 mV to −68.7 ± 0.5 mV, n = 15, $p < 0.01$) and exhibited heightened excitability reflected by an increase in the number of spikes (4.4 ± 1.6 to 14.5 ± 3.5, n = 8, $p < 0.05$) without significant alteration in input resistance (295 ± 84 to 293 ± 86 MΩ, n = 8, $p > 0.05$) (Figures 4G and 4H). This result is in agreement with a previous study, which showed that DA receptor activation increased evoked firing in fast-spiking BLA interneurons (Kröner et al., 2004).

Next, we investigated the effect of DA on cortically activated lpcs. We recorded from individual lpcs while stimulating cortical afferents in the external capsule with the stimulus strength set to evoke an EPSP large enough to fire an action potential in ~50% of the trials. Application of DA led to hyperpolarization accompanied by a significant drop in the likelihood of action potential firing (51% ± 9% before DA versus 12% ± 7% after DA, n = 4, $p < 0.05$) (Figures 4I and 4J) while leaving the evoked EPSP largely intact. This result demonstrates that DA also depresses cortically evoked action potentials in lpcs.

DA D1 Receptors Mediate the Dopaminergic Effect

We determined the DA receptor subtype that mediates the hyperpolarization caused by DA (−4.7 ± 0.4 mV, n = 20) by bath applying specific DA receptor agonists and antagonists in the presence of kynurenate (3 mM) and picrotoxin (100 μM) to isolate a direct effect on the membrane potential. The DA D1 agonist dihydrexidine, but not the DA D2 agonist quinpirole, mimicked the

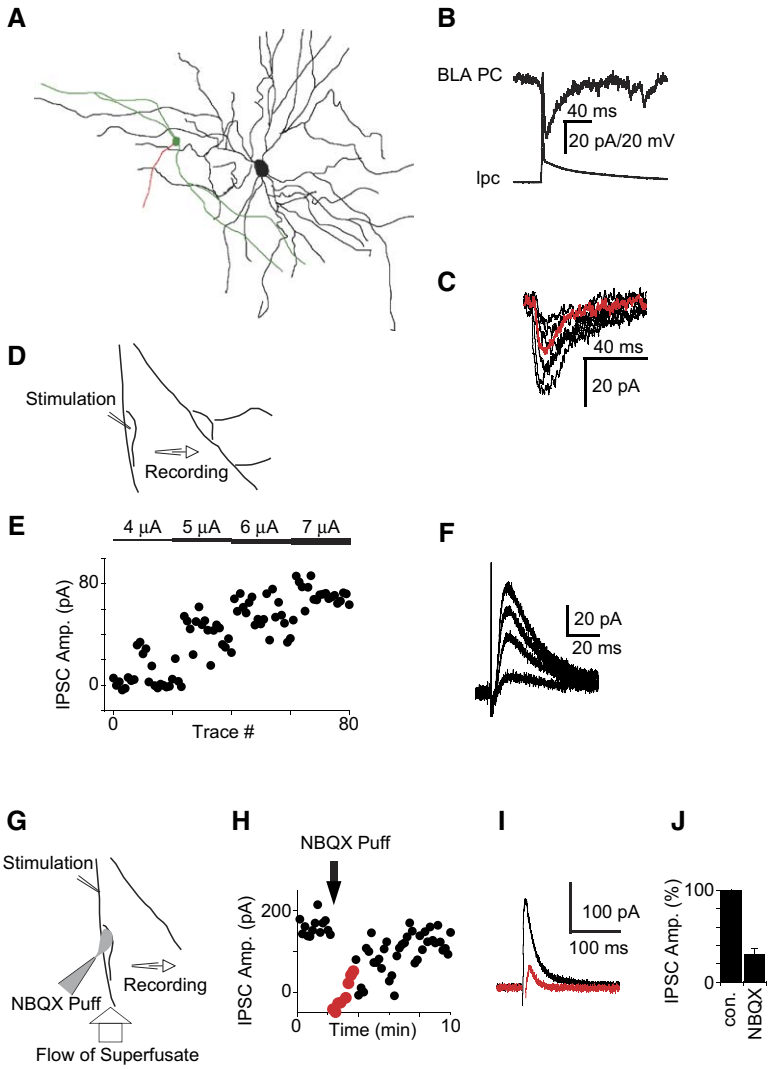

Figure 3. Lpcs Send Efferent Connections to the BLA

(A–C) Example of a paired recording between a lpc and a BLA projection neuron. (A) Both cells were filled with biocytin and subsequently stained to reveal their morphology. Soma and dendrites of the lpc are shown in green and its axon in red; soma and dendritic tree of the BLA projection neuron are shown in black. (B) Current-clamp recording from the lpc (bottom trace) and voltage-clamp recording from the BLA projection cell (top trace) in kynurenate (3 mM) to block excitatory synaptic transmission. Action potential firing in the lpc was evoked by a 1 ms long somatic current injection and was followed by a monosynaptic IPSC in the BLA projection cell, which was dialyzed with a high-chloride-containing solution, held at −60 mV, and therefore shows an inward current. (C) Overlay of individual IPSC traces illustrating the considerable trial-to-trial variability; an averaged response is shown in red.

(D–F) Individual BLA principal cells are innervated by multiple lpcs. (D) Schematic of the electrode placement. (E) Plot of IPSC amplitude recorded from a BLA-principal cell generated by extracellular stimulation in the nearby lpc cluster. The BLA projection neuron was dialyzed with a low-chloride-containing solution and held at −40 mV. Three millimolar kynurenate was added to the perfusate to block excitatory synaptic transmission. The current applied to the stimulation electrode was maintained for the times indicated by the horizontal lines and ten traces were gathered at each level. (F) Average traces measured at different stimulus strengths.

(G–J) Cortical feedforward inhibition is predominantly mediated by lpcs. (G) Placement of stimulus and recording electrodes and of the local superfusion pipette. Care was taken to place the slice such that the flow of the perfusion solution limited the area covered by the puff of NBQX. (H) Sample plot of IPSC amplitude recorded in a BLA projection cell. A 2 s puff of NBQX (1 mM) was applied at the time indicated by the downward arrow. (I) Average IPSC before (black) and during the peak effect of the NBQX puff (red). (J) Normalized IPSC amplitude before (con.) and after brief focal application of NBQX (average ± SEM, n = 5).

effects of DA on membrane potential in both lpcs and mpcs (Figure 5). Dihydrexidine (2 μM) led to a hyperpolarization of −4.4 ± 0.6 mV (n = 12, $p < 0.01$), a concomitant loss of input resistance (753 ± 51 MΩ to 532 ± 87 MΩ, n = 12, $p < 0.05$), and a decrease in the number of evoked action potentials (9.2 ± 2.0 to 4.0 ± 1.6, n = 12, $p < 0.05$) (Figures 5A and 5B). Consistently, DA combined with the DA D2 antagonist sulpiride (5 μM) hyperpolarized the resting membrane potential (−4.2 ± 1.3 mV, n = 8, $p < 0.05$), whereas quinpirole (1 μM) as well as DA together with the DA D1 antagonist SCH 23390 (5 μM) did not significantly alter the membrane potential (0.7± 0.8 mV, n = 10, $p > 0.05$ and −0.5 ± 0.8 mV, n = 9, $p > 0.05$, respectively) (Figure 5C).

DA D1 Receptors Activate GIRK Channels in pcs

DA and dihydrexidine caused a marked decrease in input resistance, suggestive of the activation of an additional membrane conductance. Classically, DA D1 receptors activate adenyl cyclase via G_s or G_{olf}, but other types of coupling, e.g., to G protein-coupled inward rectifier potassium (GIRK) channels have been observed in striatal cells (Pacheco-Cano et al., 1996). We therefore tested the hypothesis that DA activates a GIRK current in pcs. Current-voltage curves were obtained (n = 6) using a voltage ramp from −100 to −60 mV after application of picrotoxin (100 μM), kynurenate (3 mM), and TTX (1 μM). When the concentration of extracellular K^+ was 2.5 mM (recorded with K gluconate-based internal solution containing 130 mM K^+), the DA-induced current reversed at −92 ± 0.8 mV and was strongly inwardly rectifying (Figure 6A). Based on our K^+ concentrations, the K^+ reversal according to the Nernst equation would be ~−100 mV, hence the reversal potential determined by us was compatible with a K^+ current. To verify the involvement of a G protein, we

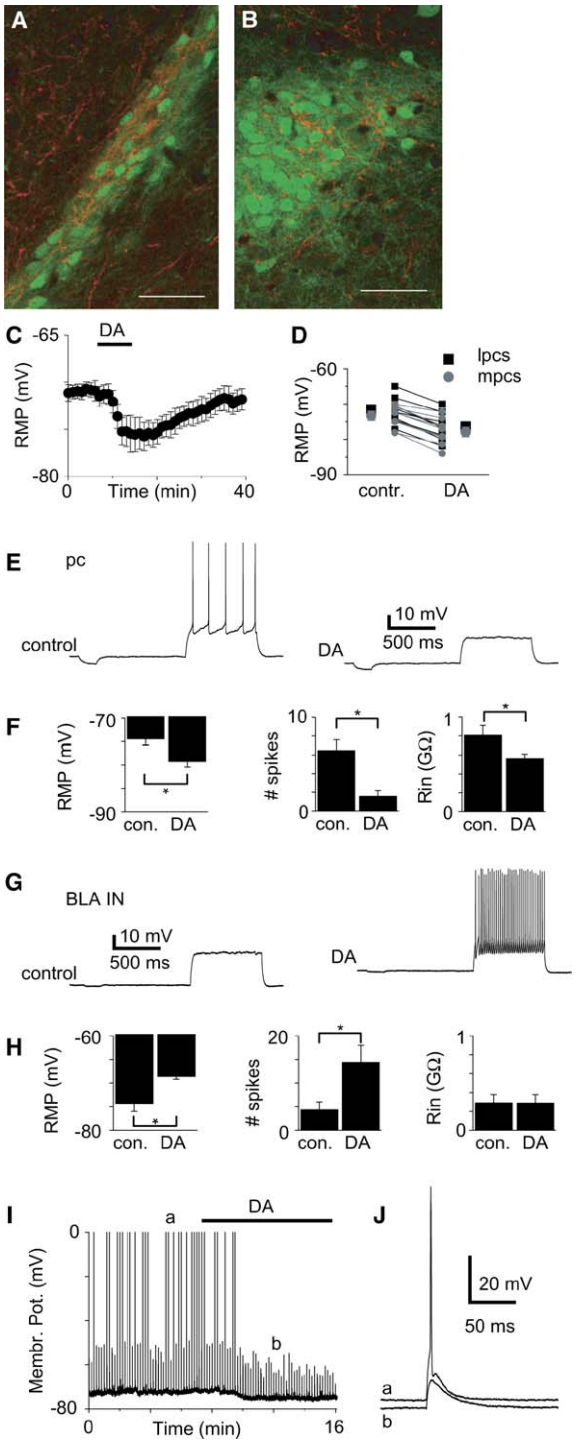

Figure 4. DA Suppresses pc Excitability and Enhances the Excitability of Classical Interneurons

(A and B) Pcs receive dense dopaminergic innervation. Confocal images of slices from GAD-GFP mice stained against tyrosine hydroxylase. Tyrosine hydroxylase-positive fibers (red) can be found within the green fluorescent clusters of lpcs (A) and mpcs (B). Scale bar: 40 μm.

(C) Current-clamp recordings of lpcs with resting membrane potential (RMP) (average ± SEM) plotted against time (n = 8). Bath application of DA (20–30 μM were used throughout the study) to the perfusate is indicated by the horizontal line.

(D) Scatter plot and averages (± SEM) of RMP of lpcs (black, n = 8) and mpcs (gray, n = 12) before (contr.) and after application of DA.

tested the effect of DA on the resting membrane potential when a blocker of G protein function, GDP-β-S (1 mM) was used in the pipette solution (n = 5). To ensure complete diffusion, cells were dialyzed with the GDP-β-S-containing solution for 25 min prior to recording. Cells were current-clamped and their resting membrane potential was monitored before and after the application of DA. DA failed to induce an inward-rectified current, suggesting that DA-induced K^+ current is G protein dependent (Figures 6B and 6C). Final evidence for the involvement of a GIRK channel was obtained by using the specific antagonist of GIRK 1/4 channels, tertiapin-Q (Figures 6D and 6E), under complete block of synaptic activity (3 mM kynurenate, 100 μM Picrotoxin, 1 μM TTX). Bath application of tertiapin-Q (1 μM) 5 min prior to either application of DA (n = 6) or dihydrexidine (2 μM) (n = 5) resulted in a complete block of hyperpolarization. These findings prove that upon activation of DA D1 receptors on pcs a GIRK 1/4 conductance is opened and leads to the observed hyperpolarization in these cells.

Presynaptic Modulation of pc Output by DA

In addition to the postsynaptic effect DA exerts on pcs, it may also influence the presynaptic release of neurotransmitter (Nicola et al., 1996). In paired recordings from lpcs and BLA principal cells (n = 3), DA hyperpolarized the presynaptic lpcs as expected. However, firing was ensured by a sufficiently large somatic current injection (Figure 7B). In the postsynaptic cell, DA led to an increase in the failure rate of the evoked IPSCs from 25.2% ± 3.2% to 86.0% ± 4.8% (n = 3, $p < 0.05$) (Figure 7A). When we averaged the success responses before and after DA for all three experiments we found a slight, albeit not significant reduction in the amplitude (14.4 ± 4.2 pA to 11.2 ± 2.5 pA, n = 3, $p > 0.5$). Given that DA does not alter the sensitivity of the $GABA_A$ receptor for GABA (Bissiere et al., 2003), this result suggested a decrease in synaptic release by DA (Figure 7C).

DA Reduces Feedforward Inhibition into the BLA and CeA

In the lateral nucleus of the amygdala, thalamically triggered feedforward inhibition is reduced in the presence of DA through activation of DA D2 receptors (Bissiere et al., 2003). Furthermore, DA excites pyramidal cells

(E) Representative current-clamp recording of a lpc, plot of the membrane potential. Response to somatic current injections (−10 pA and 40 pA) before (left) and after the application of DA (right) in the presence of kynurenic acid (3 mM) and picrotoxin (100 μM).

(F) Average (± SEM) effect of DA on RMP, the number of spikes and input resistance of pcs (n = 20).

(G) Current-clamp recording of a classical BLA interneuron, same experiment as in (E). The somatic current injection was −10 pA and 90 pA, respectively.

(H) Average (± SEM) effect of DA on RMP, the number of spikes and input resistance of BLA interneurons (n = 15).

(I) Current-clamp recording of a lpc with stimulus electrode placed onto the external capsule (see schematic in Figure 2E). Stimuli are applied every 10 s, the resulting EPSP elicits an action potential in about 50% of the cases. Application of DA (indicated by the horizontal line) results in a hyperpolarization and cessation of spiking in the lpc.

(J) Sample traces at high temporal resolution before (a) and after (b) the application of DA. Note that the EPSP size is not reduced by DA.

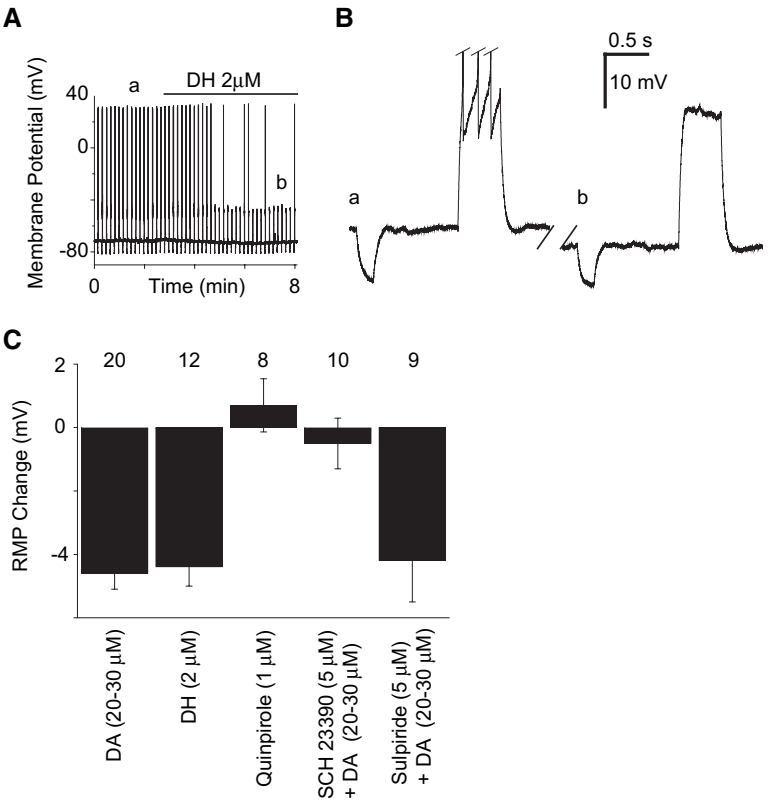

Figure 5. DA D1 Receptor Activation on pcs Mimics the DA Effect

(A) Current-clamp recording of a lpc in kynurenic acid (3 mM) and picrotoxin (100 μM). Somatic current injections of −10 pA and 50 pA were applied every 10 s. D1 receptor agonist dihydrexidine (DH) was bath-applied as indicated by the horizontal line.

(B) Sample traces at high temporal resolution before (a) and after (b) application of DH (2 μM). Action potentials are truncated.

(C) Summary of the pharmacological effects (average ± SEM) of bath-applied drugs on RMP of pcs (n indicated above the individual bars). DA, DH and DA in the presence of the DA D2 antagonist sulpiride evoked a hyperpolarizing response, whereas the DA D2 agonist quinpirole and DA in the presence of the DA D1 receptor antagonist SCH 23390 did not significantly alter the RMP of pcs.

and BLA interneurons as mentioned before, thus providing for various effects in the amygdala. How does DA affect cortically triggered feedforward inhibition, mediated by pcs, of BLA and CeA? To study this effect we placed extracellular stimulus electrodes in the lpc cluster or the mpc cluster, activating them either directly or through their excitatory synaptic input, and postsynaptic potentials consisting of an EPSP-IPSP sequence were recorded in their respective target cells (BLA pyramidal cells, CeA neurons). All target cells in BLA (Kröner et al., 2004) and CeA were depolarized by DA (7.5 ± 1.3 mV, n = 4, $p < 0.05$ and 6.3 ± 1.4 mV, n = 4, $p < 0.05$, respectively) (Figure 7D), which made it necessary to repolarize them to their original membrane potential before assessing the DAergic impact. Application of DA strongly reduced the IPSP amplitude both in CeA neurons (−4.4 ± 1.5 mV to −0.9 ± 0.7 mV, n = 4, $p < 0.05$) and BLA pyramidal cells (−5.0 ± 1.2 to −1.1 ± 0.7 mV, n = 4, $p < 0.05$) without significantly affecting the EPSP, evidenced by an unaltered initial slope (CeA cells: 4.0 ± 1.3 mV/ms to 4.2 ± 1.3 mV/ms, n = 4, $p > 0.05$; BLA projection cells: 4.7 ± 1.2 mV/ms to 4.4 ± 1.2 mV/ms, n = 4, $p > 0.05$) (Figures 7D–7G).

The reduced output of the pc system in the presence of DA may also stem from a reduced cortical input to these cells. We therefore recorded monosynaptic EPSCs in pcs evoked by stimulation of the external capsule (in case of lpcs) and either the intermediate capsule or the BLA (in case of mpcs). In lpcs, EPSC amplitudes were unaltered by DA (98% ± 8% of control, $p > 0.5$, n = 4). In contrast, a significant decrease in the EPSC amplitude was observed in mpcs when stimulating either the intermediate capsule (38% ± 4% of control, n = 4, $p < 0.05$) or the basolateral nucleus (45% ± 2% of control, n = 4, $p < 0.05$). Thus, DA reduces lpcs-mediated feedforward inhibition exclusively through direct effects on these cells, while DA exerts a compound effect on mpcs-mediated feedforward inhibition through a combination of attenuated mpc excitability and decreased cortical input. In both cases, DA strongly shifts the balance toward excitation in BLA and CeA by reducing pcs-generated inhibition and depolarizing the target cells.

D1 Receptor Activation Selectively Reduces pc Inhibitory Output

To assess more accurately the contribution of the pc system to inhibitory signals in the amygdala, we made use of their distinct DA D1 pharmacology. Given, that of all BLA interneurons only pcs are inhibited through DA D1 receptors (Kröner et al., 2004), application of the agonist dihydrexidine should reveal the fraction of inhibition these cells provide in the BLA and CeA. Target cells in the BLA or CeA were voltage-clamped in the presence of kynurenate (3 mM) (to avoid polysynaptic inhibitory responses), and monosynaptic IPSCs were evoked by stimulation of either lpcs or mpcs, respectively (Figures 8A and 8B). For BLA target cells, a second stimulus electrode was simultaneously placed inside the nucleus and control IPSCs from local interneurons were evoked (Figure 8A). Dihydrexidine (2 μM) reduced IPSCs produced both by lpc and mpc stimulation (48% ± 8% of control, n = 4, $p < 0.05$ and 60% ± 4% of control, n = 4, $p < 0.05$ respectively) but did not affect IPSCs originating from BLA interneurons (IPSC amplitude: 91% ± 11% of control, n = 4, $p > 0.4$) (Figure 8C). The DA D2 receptor agonist quinpirole (1 μM) did not affect the amplitude of

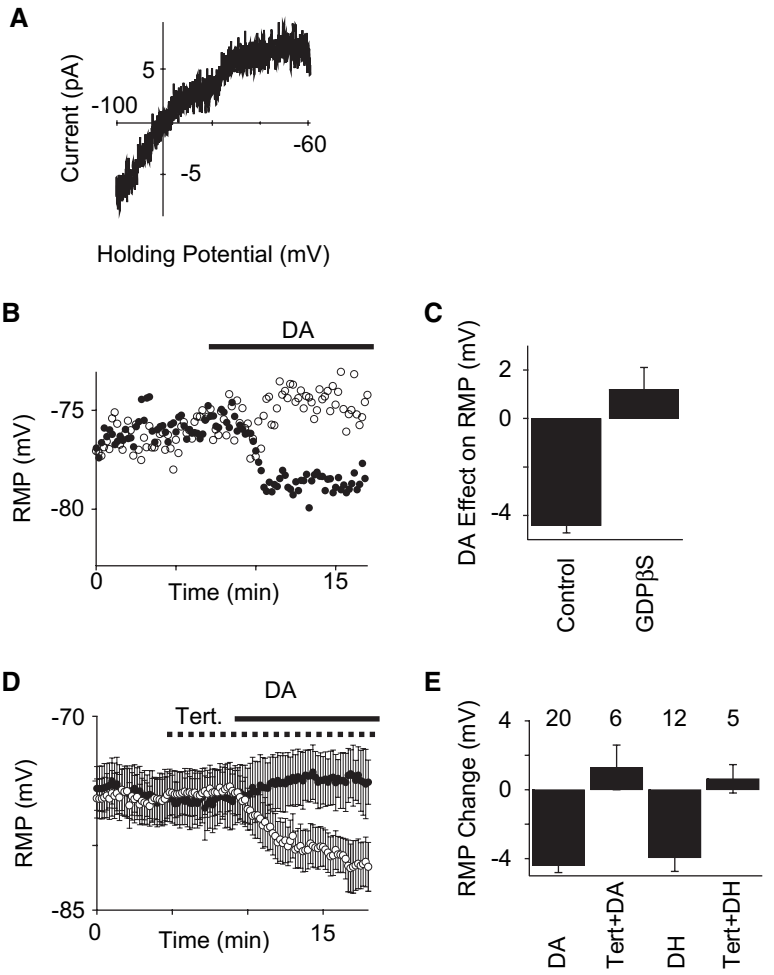

Figure 6. DA Increases a GIRK1/4 Conductance in pcs

(A) Voltage-clamp recording of a lpc with a Kgluconate-based intracellular solution. A voltage ramp from −100 to −50 mV of 1 s duration was applied in control condition and after bath application of DA. Control traces were subtracted from DA traces (average of 10–20 sweeps).

(B) Example of a current-clamp recording of pcs. The control neuron was dialyzed with normal internal solution (●), while the other cell was dialyzed with internal solution containing 1 mM GDPβS (○). DA was applied as indicated by the horizontal line.

(C) Average effect of DA on RMP of control cells (n = 20) and cells dialyzed with 1 mM GDPβS (n = 5).

(D and E) The specific GIRK1/4 antagonist tertiapine-Q blocks the hyperpolarizing effect of DA. (D) Current-clamp recordings of pcs, average (± SEM) RMP. Bath application of tertiapine-Q (1 μM) (● n = 6) 5 min prior to application of DA prevented the DA-induced hyperpolarization that was observed in control slices (○ n = 8) without pretreatment. (E) Summary graph of RMP changes after application of DA or DH (2 μM) in control slices and slices pretreated with tertiapin-Q (1 μM) (n indicated above the individual bars).

monosynaptic IPSCs produced by either lpc (99% ± 7% of control, n = 4, p > 0.5) or mpc stimulation (97% ± 6% of control, n = 4, p > 0.5) (Figures 8D and 8E).

Taken together, the output of the pc system is strongly reduced by DA through (1) loss of pc excitability resulting from the opening of a GIRK conductance, (2) a presynaptic inhibition of GABA release from pcs, and (3) in the case of mpcs but not lpcs, a concomitant decrease in excitatory cortical input.

Discussion

In the present study, we have shown that lpcs strongly resemble mpcs in physiological and functional aspects, providing evidence that the collectivity of pcs constitutes a special network of amygdala interneurons. In fact, the pc system possesses three distinctive features: (1) By virtue of its location, the pc system is ideally situated to gate incoming and outgoing information of the BLA. (2) Pcs are innervated by cortical fibers and can thus mediate cortical control in a feedforward manner over the BLA and the CeA, the two nuclei most important for triggering emotions such as fear. (3) This feed-forward network, formed by the pc system, is not rigid but rather is gated by DA acting on D1 receptors. In the presence of DA, the pc-mediated inhibition collapses, thus attenuating cortical control and most likely promoting amygdala-related behavior.

Functional Properties of pcs

Several anatomical and functional studies have demonstrated that mpcs are targeted by axons from BLA projection neurons (Krettek and Price, 1978; Pare and Smith, 1993a, 1993b) and project to cells of the CeA, providing feedforward inhibition of the CeA (Royer et al., 1999, 2000). Using paired recordings of lpcs-projection cells in acute slices, we now have demonstrated that lpcs target projection cells in the BLA and mediate cortical feedforward inhibition onto these cells. Thus, pcs control the entry into the BLA as well as the exit to the CeA. Moreover, the paired recordings revealed that lpcs form rather weak unitary connections with their postsynaptic targets, generating unitary IPSCs of less than 20 pA with the small size of the signal most likely resulting from only a few and distal synaptic contacts with dendritic cable filtering accounting for the slow kinetics.

However, a marked increase in inhibitory strength is achieved in that several lpcs target an individual BLA projection cell, evidenced by our experiments with extracellular stimulation. The result of this convergence is a substantial cortical feedforward inhibition mediated by clusters of lpcs to BLA projection cells. High tonic activity should also considerably enhance their inhibitory

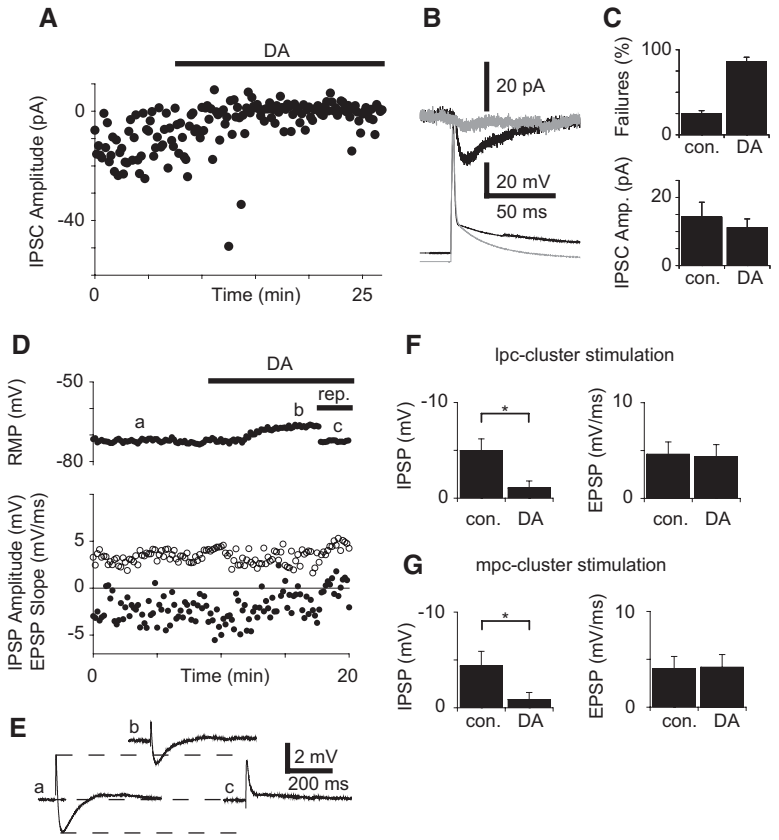

Figure 7. DA Reduces pc Output and Feedforward Inhibition of Both BLA and CeA

(A and B) Recording from a lpc-BLA projection cell pair. (A) The postsynaptic cell was recorded with a high Cl internal solution and held in voltage clamp at −60 mV in the presence of kynurenate (3 mM). DA was bath-applied as indicated by the horizontal line. (B) Average traces (10–20 events) before (black) and after (gray) the application of DA. *Top,* postsynaptic IPSCs and *bottom*, presynaptic action potential.

(C) Summary (± SEM) of the effect of DA on the IPSC failure rate and the average IPSC amplitude (failures not included) in paired recordings (n = 3).

(D–G) DA effect on pc-mediated feedforward inhibition of BLA and CeA. (D) Current-clamp recording of a BLA projection neuron. An extracellular stimulus electrode was placed onto the lpc cluster and EPSP/IPSP sequences were evoked in the postsynaptic cell. Plot of RMP (top) and of the initial EPSP slope (○) and IPSP amplitudes (●) (bottom). Initial EPSP slopes were measured instead of EPSP amplitudes to avoid contamination of the excitatory with the closely following inhibitory signal. Application of DA (horizontal line) results in a depolarization of the postsynaptic cell, which is later repolarized (rep. horizontal line) to restore the initial driving forces. (E) Sample traces from the above experiment before (a), in the presence of DA (b), and after (c) repolarizing the postsynaptic cell. (F) Average (± SEM) IPSP amplitude and initial EPSP slope in BLA projection neurons generated by lpc-cluster stimulation before and after the application of DA (n = 4). (G) Recordings from CeA neurons, synaptic potentials were evoked by a stimulus electrode placed in mpc clusters. Again, average (± SEM) IPSP amplitudes and initial EPSP slopes are plotted before and after application of DA (n = 4).

strength and was in fact observed in mpcs in vivo (Collins and Pare, 1999). In addition, Royer et al. (2000) have described a slowly deinactivating K^+ current in mpcs that keeps them in a self-sustained state of heightened excitability after episodes of suprathreshold activity. This slow afterdepolarization—that increases the likelihood that synaptic activity will trigger action potentials—was also observed in lpcs (data not shown); it is therefore reasonable to assume that lpcs possess high firing rates in vivo analogous to mpcs.

Cortical Control of pcs

A hallmark feature shared by mpcs and lpcs is their cortical activation. Cortical and in particular prefrontal cortical control over the amygdala is essential for appropriate affective response. Recent fMRI data in humans have indicated that the medial prefrontal cortex (mPFC) shapes amygdala-dependent behavior (Hariri et al., 2000, 2003) and also plays an important role in fear extinction (Phelps et al., 2004). Consequently, a disturbed interaction between the prefrontal cortex (PFC) and the amygdala is postulated to underlie the affective symptoms of psychiatric disorders such as depression (Siegle et al., 2002; Soares and Mann, 1997) and schizophrenia (Gur et al., 2002; Perlstein et al., 2003; Taylor et al., 2002).

The mPFC maintains connections to mpcs as demonstrated in various studies (Berretta et al., 2005; Freedman et al., 2000; Sesack et al., 1989; Vertes, 2004). In fact, inhibition in the CeA triggered by activation of the mPFC is thought to be mediated by mpcs (Quirk et al., 2003). Mpcs could also be excited in vivo by stimulating the perirhinal area (Collins and Pare, 1999), suggesting that at least the mpcs are influenced by more regions than just the prefrontal cortex. In contrast, detailed data on the origin of cortical fibers innervating lpcs are not available at present. Although the tract-tracing study by Vertes (2004) showed labeled fibers in the external capsule, an innervation of lpcs by these fibers was not investigated. Taking into account that feedforward inhibition triggered by mPFC afferents is strongly depressed through DA D1 receptor activation in the BLA (Rosenkranz and Grace, 2002) and cortical feedforward inhibition of the BLA is largely mediated by lpcs, we think it very likely that lpcs are also innervated by mPFC afferents.

Dopaminergic Modulation of pcs

Our finding that pcs are inhibited by DA via D1 receptors suggests a simple resolution to the paradoxical result that DA D1 receptor activation disinhibits the amygdala

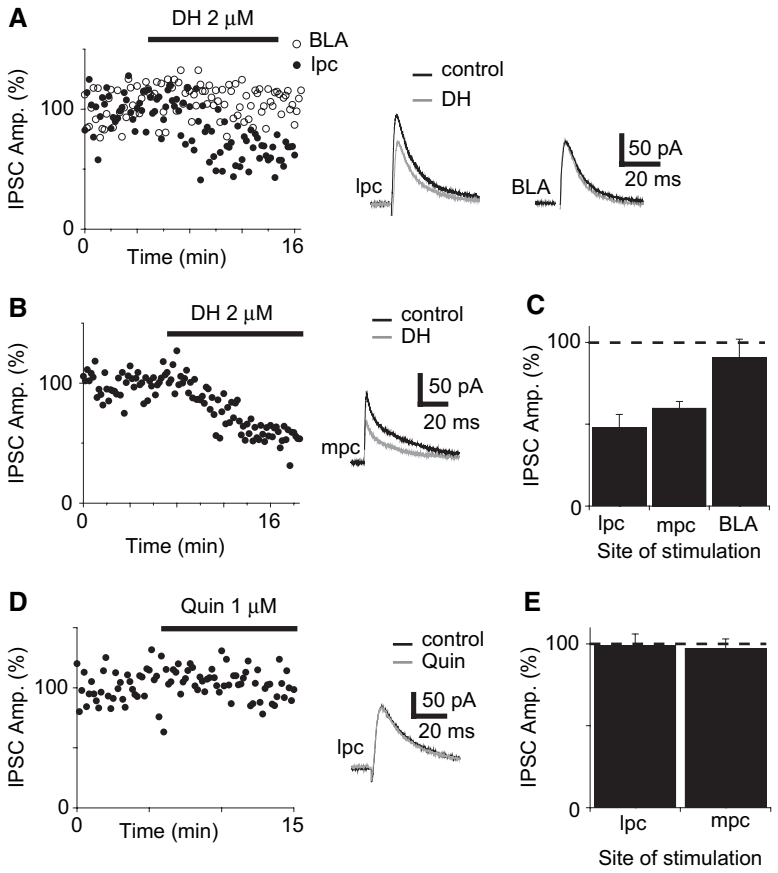

Figure 8. DA D1 Receptor Activation Reduces Inhibition Originating from pcs in the BLA and CeA

(A) Voltage-clamp recording from a BLA principal cell held at −40 mV in the presence of kynurenic acid (3 mM); one stimulus electrode was placed onto the BLA (○) and one was placed onto the lpc cluster (●). DH (2 μM) was applied as indicated by the horizontal line. *Insets:* averaged (10–20) traces before and after application of DH.

(B) Voltage-clamp recording from a neuron in the CeA; the stimulation electrode was placed in the mpc cluster. *Inset:* average traces (10–20 events) before and after the application of DH.

(C) Summary graph of the effects (± SEM) of DH on IPSC amplitudes in BLA principal cells, when stimulating in lpcs (lpc) (n = 4), in CeA neurons, when stimulating in mpcs (mpc) (n = 4), and as a control in BLA principal cells, when stimulating interneurons within the BLA (BLA) (n = 4).

(D) Voltage-clamp recording from a BLA principal cell held at −40 mV in the presence of kynurenic acid (3 mM). The stimulus electrode was placed onto the lpc cluster. Inset: averaged (10–20) traces before and after the application of quinpirole (1 μM).

(E) Summary graph of the effect (± SEM) of quinpirole on IPSC amplitudes in BLA principal cells (n = 4) and CeA neurons (n = 4).

on a systemic level yet excites classical BLA interneurons: the systemic actions of DA D1 agonists are due to disinhibition caused by silencing of the pcs network. Consistent with prior investigations showing that DA D1 receptor signaling in the amygdala does not involve the classical cAMP-dependent pathways (Leonard et al., 2003; Loretan et al., 2004), DA D1 receptors on pcs couple to GIRK channels presumably by direct interaction of βγ subunits with the GIRK1/GIRK4 channels (Huang et al., 1995). GIRK channel opening by DA D1 receptor activation has been demonstrated previously in GABAergic medium spiny neurons in the striatum (Pacheco-Cano et al., 1996), and interestingly there is evidence that these cells might be ontogenetically related to pcs (Millhouse, 1986).

Based on our results obtained in vitro, focal injection of DA D1 agonists into the amygdala should be anxiogenic in vivo, while focal application of DA D1 antagonists should result in anxiolysis. Unfortunately, DA D1 agonists have not been applied focally in behavioral tests for anxiety, but focal application of the DA D1 antagonist SCH 23390 onto mpcs in rats does indeed result in anxiolysis of the injected rats (de la Mora et al., 2005), bolstering the importance of the pc system in controlling amygdala function in vivo. Another behavioral paradigm that involves mPFC innervation and dopaminergic modulation is fear extinction, in which increased mPFC input leads to a suppression of amygdala function and fear-related behavior (Phelps et al., 2004). Interestingly, systemic application of DA D1 receptor agonists leads to a retardation and even reversal of fear extinction in the rat (Borowski and Kokkinidis, 1998), pointing to a critical involvement of the pc system in this phenomenon as well. Moreover, it was recently demonstrated that chronic stress, which likely increases dopamine levels in the amygdala (Inglis and Moghaddam, 1999; Yokoyama et al., 2005), produces disinhibition in the CeA in vivo, similar to the effect achieved by severing mPFC afferents (Correll et al., 2005). Again, the pc system is the most likely candidate for mediating this effect.

Evidently, some classical BLA interneurons are also excited by cortical afferents (Lang and Pare, 1998; Rosenkranz and Grace, 2002; Szinyei et al., 2000) and thus could putatively mediate cortical control over the BLA. But these interneurons have not been further characterized; in particular, data on to their inhibitory impact on BLA signaling are still missing. In fact, the most detailed studies available on BLA interneurons deal with the large fraction of parvalbumin-positive interneurons in the BLA (McDonald et al., 2005; Smith et al., 2000), which are innervated predominantly by local projection cells rather than cortical afferents. Furthermore, in all BLA interneurons recorded (Kröner et al., 2004), DA D1 receptor activation causes an increase in excitability. Nevertheless a DA D1 effect on the inhibitory output of BLA interneurons receiving cortical afferents cannot be ruled out altogether. First, it is possible that these BLA interneurons are not included in the subgroup of cells in which DAergic effects have been studied. Second, their cortical excitatory input might be reduced by

DA D1 receptors as suggested by Grace and Rosenkranz (2002).

In addition to cortical feedforward inhibition, the amygdala also receives afferent input and feedforward inhibition from the thalamus. Interestingly, via activation of DA D2 receptors on LA interneurons, DA depresses thalamic feedforward inhibition and thereby facilitates the induction of long-term potentiation in the lateral amygdala (Bissiere et al., 2003).

Given the interneuron-specific DAergic effects, the spatio-temporal characteristics of DA release allow for a flexible control of amygdala signaling. Low activity levels of the DAergic afferents in the amygdala will preferentially depress the output of pcs due to their dense somatic DAergic innervation. High levels of activity will cause volume transmission and additionally activate DA receptors on other neurons. In expression systems, DA D1 receptors possess a several-fold higher affinity for DA than DA D2 receptors (Seeman and Van Tol, 1994), which may explain differential activation of the receptors in vivo in certain brain regions (Trantham-Davidson et al., 2004). Again, low levels of DA release would predominantly activate DA D1 receptors, inhibit the pc system, and facilitate amygdala function, whereas stronger activation would also activate DA D2 receptors and allow for synaptic plasticity.

Experimental Procedures

GAD-GFP Mice

The generation of glutamate decarboxylase 67 (GAD67)-GFP (Δneo) mice used in the present study were described by Tamamaki et al. (2003). In brief, a cDNA-encoding EGFP was targeted to the locus encoding GAD67 using homologous recombination in order to specifically express EGFP in GAD67-positive cells of the transgenic mice because the expression of EGFP is under the control of the endogenous GAD67 promoter in the transgenic mice. Homologous recombinant ES cells were used to generate chimeric male mice. GAD67-GFP mice were obtained by breeding the chimeric male mice with C57BL/6 female mice. The GAD67-GFP mice, which retain a loxP-flanked neomycin-resistance cassette (PGK-Neo), were crossed with CAG-cre transgenic mice (Sakai and Miyazaki, 1997) to delete the PGK-neo sequences. The resultant GAD67-GFP (Δneo) mice lack the PGK-Neo cassette, and the expression of EGFP in GAD67-GFP (Δneo) mouse brain was found to be higher than that of EGFP in GAD67-GFP mouse brain (Tamamaki et al., 2003). We used the heterozygous GAD67-GFP (Δneo) mice and called these transgenic mice GAD-GFP mice for simplicity. Because the knockout of both GAD67 alleles is lethal at birth (Asada et al., 1997), mice heterozygous for the altered GAD67 allele were used for all experiments in this study.

Electrophysiology

Coronal slices (300–400 μm thick) were cut with a vibratome (Microm HM 650V, Germany) from brains of 17- to 28-day-old mice. Animals were anesthetized with isoflurane and killed by decapitation in accordance with national and institutional guidelines. Brains were quickly removed and transferred to ice-cold oxygenated (95% O2, 5% CO2) artificial cerebrospinal fluid (ACSF) containing (in mM): 125 NaCl, 26 $NaHCO_3$, 1.25 NaH_2PO_4, 2.5 KCl, 1 $MgCl_2$, 1 $CaCl_2$, and 10 glucose. Slices were cut at 4ºC, placed in 32ºC –34ºC warm ACSF for 20–30 min, and then kept at room temperature.

An upright microscope (Olympus BX51WI, Switzerland), equipped with Nomarski differential interference contrast optics, an infrared videoimaging camera (VX55 Till Photonics, Germany), and a standard 100 W tungsten lamp connected to an epifluorescence system were used to visualize EGFP-expressing interneurons in the acute slices using a 20×/0.95NA water immersion lens. Patch pipettes were pulled from borosilicate glass tubing (1.5 mm outer diameter, 1.17 mm inner diameter) (Clark, England). The pipettes had open tip resistances of 4–8 MΩ and were filled with an intracellular solution containing (in mM): 130 K gluconate, 1 EGTA, 10 HEPES, 5 Mg ATP, 0.5 Na GTP and 5 NaCl. The pH was adjusted to 7.3 with KOH, osmolarity was 290–300 mOsM. For some experiments 1 mM GDPβS was included. For paired recordings, the postsynaptic cell was patched with pipettes filled with an intracellular solution containing (in mM): 100 CsCl, 2 $MgCl_2$, 0.1 EGTA, 2 MgATP, 0.3 NaGTP, and 40 HEPES. The pH was adjusted to 7.3 with CsOH, osmolarity was 290–300 mOsM. Sometimes 2 mg/ml biocytin was added to either solution for reconstruction of the cell. The recording temperature was 30ºC–33ºC. Recordings with initial resting potentials more positive than −55 mV for interneurons and −65 mV for principal neurons were discarded.

All membrane potentials have been corrected for a junction potential of 11 mV for recordings with the potassium gluconate solution. Data were recorded with a Multiclamp 700A amplifier (Axon Instruments), filtered at 10 kHz, and digitized at 20 kHz (A/D hardware from National Instruments). In all experiments, series resistance was monitored throughout the experiment by applying a hyperpolarizing pulse, and if it changed by more than 20%, the data were not included in the analysis. Data were acquired and analyzed on standard personal computers with IGOR Pro software (Wave Metrics, Lake Oswego). Spontaneous events were detected offline with the "Mini Analysis" Program (Synaptosoft). NBQX, CGP 55485, (S)-(–)-sulpiride, dihydrexidine, SCH23390, and (–)-quinpirole were from Tocris-Cookson (ANAWA Trading, Switzerland); all other chemicals were from Fluka/Sigma (Switzerland). Statistics: multiple comparisons were performed with ANOVA and post-hoc Bonferroni tests, simple and pairwise comparisons were performed with the appropriate two-tailed Student's t tests. Results of several experiments are reported as average ± standard error of the mean (± SEM).

Immunohistochemistry

Immunoperoxidase staining for E-GFP was performed as described (Zeilhofer et al., 2005) in perfusion-fixed tissue from 3- to 4-week-old transgenic mice, using a polyclonal antibody against GFP (1:80,000; Synaptic Systems, Göttingen, Germany). No specific staining was observed in tissue from wild-type mice. For illustration, digital photomicrographs were taken with a Zeiss Axiocam camera. Double-immunofluorescence staining was performed with antibodies against GFP, against classical markers of interneurons in the amygdala (parvalbumin, calbindin, NPY, somatostatin, CCK), and against tyrosine hydroxylase (1:10'000; Diasorin, Stillwater, Minnesota) as described (Zeilhofer et al., 2005), using secondary antibodies coupled to Alexa 488 and Cy3. Images from both markers were acquired sequentially by multitracking with a Zeiss LSM 510 Meta confocal laser scanning microscope and then digitally merged. For illustration, stacks of 8–12 confocal sections spaced by 0.5 μm were generated using a maximal-intensity projection algorithm.

Colocalization of interneuron markers and GFP was assessed in single confocal sections. The pcs from four mice for this experiment were not double-labeled for any of the markers. Analysis of the distribution of TH-positive axons in the parietal cortex and hippocampus of both wild-type and transgenic revealed that presumptive noradrenergic axons were labeled only weakly at the antibody concentration used, whereas presumptive dopaminergic axons in the cingulate cortex, basal ganglia, and hypothalamus were strongly labeled. Therefore, TH-positive axons in the amygdala likely represent dopaminergic projections.

Supplemental Data

Supplemental Data include one figure and a 3D reconstruction and are available with this article online at http://www.neuron.org/cgi/content/full/48/6/1025/DC1/.

Acknowledgments

We thank Jean-Marc Fritschy, Andreas Lüthi, Anita Lüthi, Urs Gerber, Richard Mailman, Matthew Frerking, and Beat Gähwiler for their technical assistance and their critical review of the manuscript. A.M. and K.E.V. are supported by grant 631-066012 of the Swiss National Science Foundation.

Received: July 15, 2005
Revised: September 8, 2005
Accepted: October 20, 2005
Published: December 21, 2005

References

Alheid, G.F., de Olmos, J.S., and Beltramino, C.A. (1995). Amygdala and Extended Amygdala. In The Rat Nervous System, G. Paxinos, ed. (San Diego: Academic Press), pp. 495–578.

Asada, H., Kawamura, Y., Maruyama, K., Kume, H., Ding, R.G., Kanbara, N., Kuzume, H., Sanbo, M., Yagi, T., and Obata, K. (1997). Cleft palate and decreased brain gamma-aminobutyric acid in mice lacking the 67-kDa isoform of glutamic acid decarboxylase. Proc. Natl. Acad. Sci. USA *94*, 6496–6499.

Asan, E. (1998). The catecholaminergic innervation of the rat amygdala. Adv. Anat. Embryol. Cell Biol. *142*, 1–118.

Berretta, S., Pantazopoulos, H., Caldera, M., Pantazopoulos, P., and Pare, D. (2005). Infralimbic cortex activation increases c-Fos expression in intercalated neurons of the amygdala. Neuroscience *132*, 943–953.

Bissiere, S., Humeau, Y., and Luthi, A. (2003). Dopamine gates LTP induction in lateral amygdala by suppressing feedforward inhibition. Nat. Neurosci. *6*, 587–592.

Borowski, T.B., and Kokkinidis, L. (1998). The effects of cocaine, amphetamine, and the dopamine D1 receptor agonist SKF 38393 on fear extinction as measured with potentiated startle: implications for psychomotor stimulant psychosis. Behav. Neurosci. *112*, 952–965.

Collins, D.R., and Pare, D. (1999). Spontaneous and evoked activity of intercalated amygdala neurons. Eur. J. Neurosci. *11*, 3441–3448.

Correll, C.M., Rosenkranz, J.A., and Grace, A.A. (2005). Chronic cold stress alters prefrontal cortical modulation of amygdala neuronal activity in rats. Biol. Psychiatry *58*, 382–391.

de la Mora, M.P., Cardenas-Cachon, L., Vazquez-Garcia, M., Crespo-Ramirez, M., Jacobsen, K., Höistad, M., Agnati, L.F., and Fuxe, K. (2005). Anxiolytic effects of intra-amygdaloid injection of the D1 antagonist SCH23390 in the rat. Neurosci. Lett. *377*, 101–105.

Freedman, L.J., Insel, T.R., and Smith, Y. (2000). Subcortical projections of area 25 (subgenual cortex) of the macaque monkey. J. Comp. Neurol. *421*, 172–188.

Fuxe, K., Jacobsen, K.X., Hoistad, M., Tinner, B., Jansson, A., Staines, W.A., and Agnati, L.F. (2003). The dopamine D1 receptor-rich main and paracapsular intercalated nerve cell groups of the rat amygdala: relationship to the dopamine innervation. Neuroscience *119*, 733–746.

Grace, A.A., and Rosenkranz, J.A. (2002). Regulation of conditioned responses of basolateral amygdala neurons. Physiol. Behav. *77*, 489–493.

Greba, Q., and Kokkinidis, L. (2000). Peripheral and intraamygdalar administration of the dopamine D1 receptor antagonist SCH 23390 blocks fear-potentiated startle but not shock reactivity or the shock sensitization of acoustic startle. Behav. Neurosci. *114*, 262–272.

Gur, R.E., McGrath, C., Chan, R.M., Schroeder, L., Turner, T., Turetsky, B.I., Kohler, C., Alsop, D., Maldjian, J., Ragland, J.D., and Gur, R.C. (2002). An fMRI study of facial emotion processing in patients with schizophrenia. Am. J. Psychiatry *159*, 1992–1999.

Hariri, A.R., Bookheimer, S.Y., and Mazziotta, J.C. (2000). Modulating emotional responses: effects of a neocortical network on the limbic system. Neuroreport *11*, 43–48.

Hariri, A.R., Mattay, V.S., Tessitore, A., Fera, F., and Weinberger, D.R. (2003). Neocortical modulation of the amygdala response to fearful stimuli. Biol. Psychiatry *53*, 494–501.

Huang, C.L., Slesinger, P.A., Casey, P.J., Jan, Y.N., and Jan, L.Y. (1995). Evidence that direct binding of G beta gamma to the GIRK1 G protein-gated inwardly rectifying K+ channel is important for channel activation. Neuron *15*, 1133–1143.

Humeau, Y., Shaban, H., Bissiere, S., and Luthi, A. (2003). Presynaptic induction of heterosynaptic associative plasticity in the mammalian brain. Nature *426*, 841–845.

Inglis, F.M., and Moghaddam, B. (1999). Dopaminergic innervation of the amygdala is highly responsive to stress. J. Neurochem. *72*, 1088–1094.

Inoue, T., Izumi, T., Maki, Y., Muraki, I., and Koyama, T. (2000). Effect of the dopamine D(1/5) antagonist SCH 23390 on the acquisition of conditioned fear. Pharm Biochem. Behav. *66*, 573–578.

Krettek, J.E., and Price, J.L. (1978). Amygdaloid projections to subcortical structures within the basal forebrain and brainstem in the rat and cat. J. Comp. Neurol. *178*, 225–254.

Kröner, S., Rosenkranz, A.J., Grace, A.A., and Barrionuevo, G. (2004). Dopamine modulates excitability of basolateral amygdala neurons in vitro. J. Neurophysiol. *843*, 1–48.

Lamont, E.W., and Kokkinidis, L. (1998). Infusion of the dopamine D1 receptor antagonist SCH 23390 into the amygdala blocks fear expression in a potentiated startle paradigm. Brain Res. *795*, 128–136.

Lang, E.J., and Pare, D. (1998). Synaptic responsiveness of interneurons of the cat lateral amygdaloid nucleus. Neuroscience *83*, 877–889.

Le Gal LaSalle, G., Paxinos, G., and Ben-Ari, Y. (1978). Neurochemical mapping of GABAergic systems in the amygdaloid complex and bed nucleus of the stria terminalis. Brain Res. *155*, 397–403.

LeDoux, J.E. (2000). Emotion circuits in the brain. Annu. Rev. Neurosci. *23*, 155–184.

Leonard, S.K., Anderson, C.M., Lachowicz, J.E., Schulz, D.W., Kilts, C.D., and Mailman, R.B. (2003). Amygdaloid D1 receptors are not linked to stimulation of adenylate cyclase. Synapse *50*, 320–333.

Loretan, K., Bissiere, S., and Luthi, A. (2004). Dopaminergic modulation of spontaneous inhibitory network activity in the lateral amygdala. Neuropharmacology *47*, 631–639.

McDonald, A.J., Mascagni, F., Mania, I., and Rainnie, D.G. (2005). Evidence for a perisomatic innervation of parvalbumin-containing interneurons by individual pyramidal cells in the basolateral amygdala. Brain Res. *1035*, 32–40.

Meloni, E.G., and Davis, M. (1999). Enhancement of the acoustic startle response in rats by the dopamine D1 receptor agonist SKF 82958. Psychopharmacology (Berl.) *144*, 373–380.

Millhouse, O.E. (1986). The intercalated cells of the amygdala. J. Comp. Neurol. *247*, 246–271.

Missale, C., Nash, S.R., Robinson, S.W., Jaber, M., and Caron, M.G. (1998). Dopamine receptors: from structure to function. Physiol. Rev. *78*, 189–225.

Nader, K., and LeDoux, J.E. (1999). Inhibition of the mesoamygdala dopaminergic pathway impairs the retrieval of conditioned fear associations. Behav. Neurosci. *113*, 891–901.

Nicola, S.M., Kombian, S.B., and Malenka, R.C. (1996). Psychostimulants depress excitatory synaptic transmission in the nucleus accumbens via presynaptic D1-like dopamine receptors. J. Neurosci. *16*, 1591–1604.

Pacheco-Cano, M.T., Bargas, J., Hernandez-Lopez, S., Tapia, D., and Galarraga, E. (1996). Inhibitory action of dopamine involves a subthreshold Cs(+)-sensitive conductance in neostriatal neurons. Exp. Brain Res. *110*, 205–211.

Pare, D., and Smith, Y. (1993a). Distribution of GABA immunoreactivity in the amygdaloid complex of the cat. Neuroscience *57*, 1061–1076.

Pare, D., and Smith, Y. (1993b). The intercalated cell masses project to the central and medial nuclei of the amygdala in cats. Neuroscience *57*, 1077–1090.

Pare, D., Royer, S., Smith, Y., and Lang, E.J. (2003). Contextual inhibitory gating of impulse traffic in the intra-amygdaloid network. Ann. N Y Acad. Sci. *985*, 78–91.

Perlstein, W.M., Dixit, N.K., Carter, C.S., Noll, D.C., and Cohen, J.D. (2003). Prefrontal cortex dysfunction mediates deficits in working memory and prepotent responding in schizophrenia. Biol. Psychiatry *53*, 25–38.

Phelps, E.A., Delgado, M.R., Nearing, K.I., and LeDoux, J.E. (2004). Extinction learning in humans: role of the amygdala and vmPFC. Neuron *43*, 897–905.

Quirk, G.J., Likhtik, E., Pelletier, J.G., and Pare, D. (2003). Stimulation of medial prefrontal cortex decreases the responsiveness of central amygdala output neurons. J. Neurosci. *23*, 8800–8807.

Rosenkranz, J.A., and Grace, A.A. (1999). Modulation of basolateral amygdala neuronal firing and afferent drive by dopamine receptor activation in vivo. J. Neurosci. *19*, 11027–11039.

Rosenkranz, J.A., and Grace, A.A. (2002). Cellular mechanisms of infralimbic and prelimbic prefrontal cortical inhibition and dopaminergic modulation of basolateral amygdala neurons in vivo. J. Neurosci. *22*, 324–337.

Royer, S., Martina, M., and Pare, D. (1999). An inhibitory interface gates impulse traffic between the input and output stations of the amygdala. J. Neurosci. *19*, 10575–10583.

Royer, S., Martina, M., and Pare, D. (2000). Bistable behavior of inhibitory neurons controlling impulse traffic through the amygdala: role of a slowly deinactivating K+ current. J. Neurosci. *20*, 9034–9039.

Sakai, K., and Miyazaki, J. (1997). A transgenic mouse line that retains Cre recombinase activity in mature oocytes irrespective of the cre transgene transmission. Biochem. Biophys. Res. Commun. *237*, 318–324.

Sanders, S.K., and Shekhar, A. (1995). Regulation of anxiety by GABAA receptors in the rat amygdala. Pharmacol. Biochem. Behav. *52*, 701–706.

Seeman, P., and Van Tol, H.H. (1994). Dopamine receptor pharmacology. Trends Pharmacol. Sci. *15*, 264–270.

Sesack, S.R., Deutch, A.Y., Roth, R.H., and Bunney, B.S. (1989). Topographical organization of the efferent projections of the medial prefrontal cortex in the rat: an anterograde tract-tracing study with Phaseolus vulgaris leucoagglutinin. J. Comp. Neurol. *290*, 213–242.

Siegle, G.J., Steinhauer, S.R., Thase, M.E., Stenger, V.A., and Carter, C.S. (2002). Can't shake that feeling: event-related fMRI assessment of sustained amygdala activity in response to emotional information in depressed individuals. Biol. Psychiatry *51*, 693–707.

Smith, Y., and Pare, D. (1994). Intra-amygdaloid projections of the lateral nucleus in the cat: PHA-L anterograde labeling combined with postembedding GABA and glutamate immunocytochemistry. J. Comp. Neurol. *342*, 232–248.

Smith, Y., Pare, J.F., and Pare, D. (2000). Differential innervation of parvalbumin-immunoreactive interneurons of the basolateral amygdaloid complex by cortical and intrinsic inputs. J. Comp. Neurol. *416*, 496–508.

Soares, J.C., and Mann, J.J. (1997). The anatomy of mood disorders–review of structural neuroimaging studies. Biol. Psychiatry *41*, 86–106.

Szinyei, C., Heinbockel, T., Montagne, J., and Pape, H.C. (2000). Putative cortical and thalamic inputs elicit convergent excitation in a population of GABAergic interneurons of the lateral amygdala. J. Neurosci. *20*, 8909–8915.

Tamamaki, N., Yanagawa, Y., Tomioka, R., Miyazaki, J., Obata, K., and Kaneko, T. (2003). Green fluorescent protein expression and colocalization with calretinin, parvalbumin, and somatostatin in the GAD67-GFP knock-in mouse. J. Comp. Neurol. *467*, 60–79.

Taylor, S.F., Liberzon, I., Decker, L.R., and Koeppe, R.A. (2002). A functional anatomic study of emotion in schizophrenia. Schizophr. Res. *58*, 159–172.

Trantham-Davidson, H., Neely, L.C., Lavin, A., and Seamans, J.K. (2004). Mechanisms underlying differential D1 versus D2 dopamine receptor regulation of inhibition in prefrontal cortex. J. Neurosci. *24*, 10652–10659.

Vertes, R.P. (2004). Differential projections of the infralimbic and prelimbic cortex in the rat. Synapse *51*, 32–58.

Yokoyama, M., Suzuki, E., Sato, T., Maruta, S., Watanabe, S., and Miyaoka, H. (2005). Amygdalic levels of dopamine and serotonin rise upon exposure to conditioned fear stress without elevation of glutamate. Neurosci. Lett. *379*, 37–41.

Zeilhofer, H.U., Studler, B., Arabadzisz, D., Schweizer, C., Ahmadi, S., Layh, B., Bösl, M.R., and Fritschy, J.-M. (2005). Glycinergic neurons expressing EGFP in BAC transgenic mice. J. Comp. Neurol. *482*, 123–141.